Chemistry and Physics of Lipids 236 (2021) 105063

Contents lists available at ScienceDirect

Chemistry and Physics of Lipids

journal homepage: www.elsevier.com/locate/chemphyslip

Multisite interactions of prions with membranes and native nanodiscs

Michael Overduin [a,*], Holger Wille [a,b], David Westaway [a,b]

[a] Department of Biochemistry, University of Alberta, Edmonton, Alberta, Canada
[b] Center for Prions and Protein Folding Diseases, University of Alberta, Edmonton, Alberta, Canada

ARTICLE INFO

Keywords:
Amyloid
Membrane protein
Memtein
Native nanodisc
Prion
Neurodegenerative disease
Scrapie
Styrene maleic acid
SMALP

ABSTRACT

Although prions are known as protein-only infectious particles, they exhibit lipid specificities, cofactor dependencies and membrane-dependent activities. Such membrane interactions play key roles in how prions are processed, presented and regulated, and hence have significant functional consequences. The expansive literature related to prion protein interactions with lipids and native nanodiscs is discussed, and provides a unique opportunity to re-evaluate the molecular composition and mechanisms of its infectious and cellular states. A family of crystal and solution structures of prions are analyzed here for the first time using the membrane optimal docking area (MODA) program, revealling the presence of structured binding elements that could mediate specific lipid recognition. A set of motifs centerred around W99, L125, Y169 and Y226 are consistently predicted as being membrane interactive and form an exposed surface which includes α helical, β strand and loop elements involving the prion protein (PrP) structural domain, while the scrapie form is radically different and doubles the size of the membrane interactive site into an extensible surface. These motifs are highly conserved throughout mammalian evolution, suggesting that prions have long been intrinsically attached to membranes at central and N- and C-terminal points, providing several opportunities for stable and specific bilayer interactions as well as multiple complexed orientations. Resistance or susceptibility to prion disease correlates with increased or decreased membrane binding propensity by mutant forms, respectively, indicating a protective role by lipids. The various prion states found *in vivo* are increasingly resolvable using native nanodiscs formed by styrene maleic acid (SMA) and stilbene maleic acid (STMA) copolymers rather than classical detergents, allowing the endogenous states to be tackled. These copolymers spontaneously fragment intact membranes into water-soluble discs holding a section of native bilayer, and can accommodate prion multimers and mini-fibrils. Such nanodiscs have also proven useful for understanding how β amyloid and α synuclein proteins contribute to Alzheimer's and Parkinson's diseases, providing further biomedical applications. Structural and functional insights of such proteins in styrene maleic acid lipid particles (SMALPs) can be resolved at high resolution by methods including cryo-electron microscopy (cEM), motivating continued progress in polymer design to resolve biological and pathological mechanisms.

1. Introduction

Numerous diseases have developed that debilitate neurons through protein aggregation phenomena and lead to cognitive loss and eventual death. They are exemplified by sporadic Creutzfeldt–Jakob disease (CJD), which manifests biologically as neuronal loss, astrogliosis, spongiosis, and clinically as ataxia, dementia and myoclonus. Our ability to design therapeutic or preventative measures to counter such conditions has been blunted by our limited ability to identify, separate, visualize and manipulate the causative agents of disease progression. This is due in large part to the complex nature of these targets. They are heterogeneous, bearing multiple post-translational modifications and cleavage sites, and they interact with many cellular partners including soluble and transmembrane proteins, cofactors and lipids. They also exhibit dynamic behaviour, forming a diversity of conformational, oligomeric and fibrillar states depending on where they exist in cell signaling and processing pathways and stages of disease progression.

New tools are emerging to address the challenges presented, including amphipathic polymers that can be used to solubilize membrane assemblies directly from endogenous tissues into native nanodiscs for structure-function analysis without compromising biological integrity (Overduin and Esmaili, 2019a). This contrasts with detergents that

* Corresponding author.
E-mail address: overduin@ualberta.ca (M. Overduin).

https://doi.org/10.1016/j.chemphyslip.2021.105063
Received 3 November 2020; Received in revised form 29 January 2021; Accepted 12 February 2021
Available online 15 February 2021

typically destroy lipid bilayers, obliterating their native asymmetric states and displacing lipid ligands, all the while destabilizing, altering or deactivating most attached proteins. Unlike nanodiscs formed using other wrappers such as membrane scaffold proteins (MSPs), SMALPs require no detergent at any stage, contain no confounding protein signals or liabilities such as reactive or unstable moieties, and production can be cost-effectively scaled to the kg level for therapeutic and diagnostic targets (Overduin and Esmaili, 2019b).

The transient oligomeric intermediates of amyloid and prion proteins are fragile but once purified intact can be resolved by NMR, mass spectrometry and single particle methods including cEM, fluorescence and atomic force spectroscopy. The biologically intact membrane bound states are key for toxicity, although the specific lipids involved are typically unclear (Cawood et al., 2021). Computational methods are being developed for predicting novel lipid bilayer interaction sites interactions, such as the MODA program (Kufareva et al., 2014). Here these tools are employed to gain insights into prion mechanisms within the asymmetric cellular membranes they normally reside in, leading to the proposal that prions in their native environment are necessarily membrane:protein assemblies or memteins (Overduin and Esmaili, 2019a) rather than protein-only particles.

2. Evidence for prion:lipid interactions

The cellular prion protein (PrP^C) is most abundant in the central nervous system (CNS) (Acevedo-Morantes and Wille, 2014), and is generally associated with the cell surface by associations with the plasma membrane. Its biological function, however, remains unclear. Suggested roles and activities are diverse and include control over neurite outgrowth (Kanaani et al., 2005), interaction with Cu^{2+} ions and modulation of redox processes (see below), blunting entry into apoptosis (Bounhar et al., 2001), mediating synaptotoxicity in response to Aβ oligomers (Lauren et al., 2009), activation of a G-protein coupled receptor (GPCR) in the peripheral nervous system (Kuffer et al., 2016) and contributing to learning and memory processes in zebrafish (Leighton et al., 2018). A clearer definition of prion function depends on a deeper understanding of its molecular structure and interactions, which remain obscure due to the multiple states, dynamics and heterogeneity.

Here we argue that prions attach to membranes *via* a multiplicity of elements, which could cooperate to mediate high avidity, constitutive and specific tethering to lipid bilayers. The structure of the mature PrP^C protein includes a flexible N-terminus followed by a hydrophobic region and a globular PrP domain (Fig. 1), which exhibit membrane binding propensities as discussed below. Its independently folded structural domain would be most likely to ensure specificity for ligand binding functions and is composed of three α-helices and two β strands with exposed glycosylations at Asn^{181} and Asn^{197} and a disulfide bond linking cysteines 179 and 214 (Riek et al., 1996) (Fig. 2). The C-terminus of the protein is tethered into lipid rafts through a glycosylphosphatidylinositol (GPI) anchor (Stahl et al., 1987, 1992). Processing in the endoplasmic reticulum (ER) involves removal of the N-terminal signal peptide and C-terminal GPI anchor addition signal followed by attachment of the GPI anchor. The PrP^C product traffics through the Golgi network and is transported to the plasma membrane, where it inserts into the outer leaflet of the plasma membrane *via* the GPI moiety (Godsave et al., 2008). Smaller amounts of two alternative topologic forms called Ntm- and Ctm-PrP can be generated within the biosynthetic pathway of the ER; they share the same membrane spanning region derived from PrP's central tract of hydrophobic residues, but they are oriented in opposite ways (Yost et al., 1990). Two asparagine residues are the sites of addition of heterogeneous antennary glycosyl structures (Haraguchi et al., 1989). A further form of PrP is shed from cell, resulting from the action of ADAM10, a metalloprotease sheddase. While endoproteolytic maturation at a central site to create an abundant and metabolically stable C-terminal fragment denoted C1 was once also attributed to ADAM10, this relationship is not supported by genetic data, while the chemical processes that generate a C-terminal fragment denoted C2 have also proven difficult to decipher (Glatzel et al., 2015). In terms of ligands, several laboratories have described interactions of Cu^{2+} ions *via* four tandem binding sites in histidine-containing octarepeats, with "site 5" with encompassing histidines 96 and 111 in human PrP, and more recently interactions with histidine residues within the globular domain itself (Schilling et al., 2020). Altogether PrP^C assumes a diverse array of states, presenting a maze of possibilities for identifying the crucial states responsible for biological function and disease progression.

The infection-associated isoform of the prion protein is richer in β content (Pan et al., 1993). These progressive degenerative brain disorders in humans include CJD, fatal familial insomnia, kuru and Gerstmann–Straüssler–Scheinker (GSS) diseases, and, in other mammals, include bovine spongiform encephalopathy, chronic wasting disease and scrapie (Watts and Prusiner, 2017). Oligomers of prion proteins are thought to be the toxic forms rather than monomers or fibrils, and present hydrophobic surfaces that may insert into membranes while inducing destabilization (Simoneau et al., 2007). The infectious prion protein cannot be released from the membrane through cleavage with phosphatidylinositol-specific phospholipase C (PI-PLC), while PrP^C is readily cleaved and released (Stahl et al., 1990). Denaturation of the infectious conformer eliminates this PI-PLC blockage and demonstrates a membrane association that goes beyond the GPI anchor insertion. How membrane interaction preserves prion structural integrity or facilitates conversion remains unclear, although the identities of the lipids that could play roles are emerging.

Several lipids are known to associate with prions, although the real cofactor *in vivo* remains unclear. Galactosylceramide and sphingomyelin are found in prion rods purified from scrapie-infected Syrian hamster brains (Klein et al., 1998). Raft membranes contain cholesterol, which appears to preferentially stabilize prion multimers and may be required for degradation of PrP^C and efficient formation of PrP^{Sc} (Taraboulos et al., 1995), while reduction of sphingolipids levels increases PrP^{Sc} formation (Naslavsky et al., 1999). Interactions of recombinant prion with lipopolysaccharide (Saleem et al., 2014), phosphatidic acid (Haigh

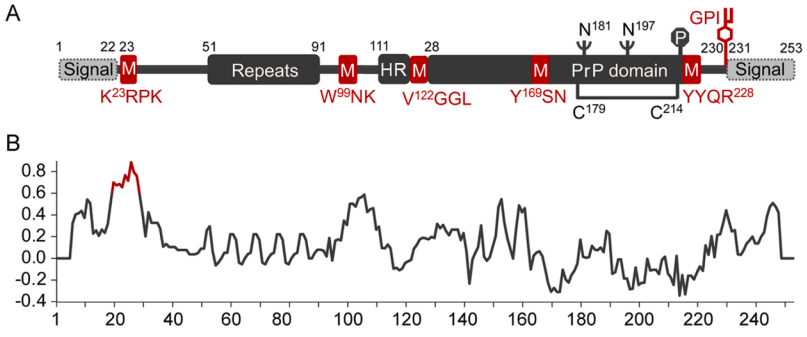

Fig. 1. Architecture of the Human Prion Protein. A) Conserved membrane interaction motifs (M) are indicated in red and include a pair of basic sequences in the flexible N-terminal region, three membrane interaction elements predicted in the prion structural domain (PrP), as well as the C-terminal GPI anchor. These proteins also contain a putative membrane-spanning hydrophobic region (HR) as well as Cu^{2+}-binding octapeptide repeats, two disulfide-forming cysteines and glycosylation sites at Asn^{181} and Asn^{197}. B) Basic-hydrophobic plot of the human prion protein sequence using the BH program (Brzeska et al., 2010) with a window size of 11, identifying a membrane interacting motif at the extreme N-terminus once the signal sequences are cleaved. Beginning with the first residue in the protein sequence, this averages the basic-hydrophobicity values for each amino acid in a segment and gives that value as the score for the middle residue in the segment.

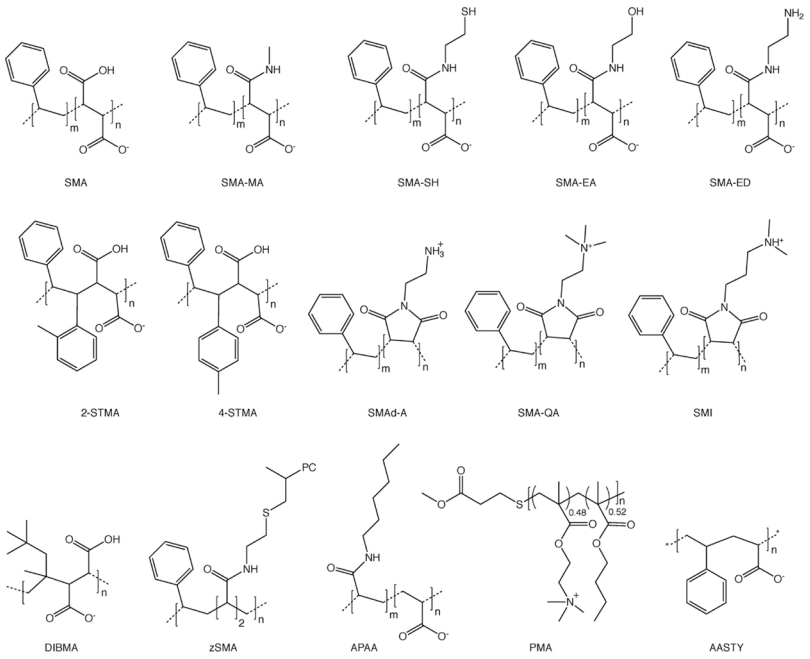

Fig. 2. Synthetic copolymers used for the solubilization of membrane-associated proteins into nanodiscs. These copolymers include styrene-*co*-maleic acid (SMA) (Knowles et al., 2009), styrene-*alt*-maleamic acid (SMA-MA) (Esmaili et al., 2020b), SMA with sulfhydrils (SMA-SH) (Lindhoud et al., 2016), SMA ethanolamine (SMA-EA) (Ravula et al., 2017b), SMA ethylenediamine (SMA-ED) (Ravula et al., 2017a), 2-methyl poly(stilbene-alt-maleic anhydride) (2-STMA), 4-methyl poly(stilbene-alt-maleic anhydride) (4-STMA) (Esmaili et al., 2020a), dehydrated SMA ethylenediamine copolymer (SMAd-A) (Ravula et al., 2017a), styrene maleimide quaternary ammonium (SMA-QA) (Ravula et al., 2018), styrene-co-maleimide (SMI) (Hall et al., 2018), diisobutylene-*alt*-maleic acid (DIBMA) (Oluwole et al., 2017), zwitterionic SMA (zSMA) (Fiori et al., 2017), alkyl polyacrylic acid (APAA) (Hardin et al., 2019), polymethacrylate (PMA) (Yasuhara et al., 2017) and acrylic acid-*co*-styrene (AASTY) (Smith et al., 2020).

et al., 2015), phosphatidylglycerol (Miller et al., 2013) and phosphatidylserine (PS) (Morillas et al., 1999; Luhrs et al., 2006) are apparent, the latter in a pH-dependent manner. Phosphatidylglycerol binding induces a shift to a more β-sheet rich structure in prions, while the ganglioside GM1 binds to the helical domain of the hamster form with its saccharide moiety being recognized by a surface encompassing the Val^{166}, Asn^{170}, Gln^{219}, Ser^{222} and Tyr^{225} residues based on docking simulations (Sanghera et al., 2011). The interaction with GM1 ganglioside induces structural changes and reduced helicity (Botto et al., 2014), and is strongest at endocytic pH values where the helical structure becomes destabilized (Re et al., 2008). The GM1 ganglioside also co-purifies with the infectious prion protein conformer, requiring additional separation steps during its purification (Levine et al., 2015). Despite identification of candidate lipid binders and sites, there remains a need to validate the endogenous ligands, specific determinants and conformational changes that convert PrP into the form that leads to transmissible propagation and neuronal dysfunction. While deposition of PrP^{Sc} correlates with degeneration of neuronal axon termini and loss of dendritic spines, destabilization of the plasmalemma and inability to maintain long-term potentiation (Belichenko et al., 2000), the mechanism of how the protein operates on biological lipid bilayers clearly requires better illumination.

Resolution of how prion proteins behave on membranes could address the longstanding hypothesis that scrapie is an inherently membrane-dependent phenomenon (Gibbons and Hunter, 1967). This concept is supported by the profiles of the sensitivity of the infectious prion particle to ionizing radiation (Latarjet et al., 1970) and oxygen (Alper et al., 1978), which match those of a membrane entity. Consideration of these data led to a revised membrane hypothesis whereby both the membrane and associated prion protein are components of the infectious agent (Alper, 1993). Yet the idea that prions are necessarily and constitutively lipid-bound may not have received the attention it deserves, although further support is building through the advent of polymer-based native nanodiscs and new structural and functional insights.

3. Polymers developed to isolate native prions and memteins

Membranes are integral to the development of neurological diseases, and may be reduced to their fundamental functional units using a specialized set of amphiphilic copolymers that convert cell membranes into nanodiscs. Hundreds of membrane proteins containing between 1 and 48 membrane-spanning helices have been isolated using styrene maleic acid lipid particles (SMALPs) from various cell types (Lee et al., 2016) since discovery that SMA polymers spontaneously liberate functionally intact membrane:protein complexes into soluble 10 nm discs (Knowles et al., 2009).

The potential of the SMALP system was demonstrated in the case of the endogenous Alternative Complex III structure, which had proven elusive using detergents but could be solubilized intact with SMA(2:1) copolymer. This allowed its six subunits, bound cofactors, post-translational modifications and attached lipids to be visualized at high resolution by cEM (Sun et al., 2018). Tackling the more heterogeneous *in vivo* prion states found in brain involved comparison of several co-polymers including the most widely used SMA copolymers which are made with non-alternating ratios of styrene to maleic acid subunits of between 2:1 and 3:1 (Esmaili et al., 2020b) (Fig. 3). The native nanodiscs formed with these copolymers were able to solubilize active prions effectively based on immunoblots and displayed the expected glycoforms, membrane-associated prion fibrils and infectious activity upon injection into rodents. For comparison a sulfhydryl containing SMA derivative (SMA-SH) (Lindhoud et al., 2016) also yielded 2D crystals of the purified prions as seen by EM (Esmaili et al., 2020b), indicating in the capacity for facilitating tight, regular packing of the nanodiscs.

A methylamine derivative of an alternating SMA(1:1) copolymer was designed in order to gently solubilize the critical prion oligomers and associated lipids into more homogeneous nanodiscs. This new copolymer, SMA-MA (Fig. 3), is more tolerant of polyvalent-cations and had proven useful for solubilizing Ca^{2+}-dependent daptomycin tetramers and octamers (Beriashvili et al., 2020). It better preserves prion oligomers, as resolved by sucrose density ultracentrifugation, and forms larger nanoparticles that retain at least twice as much lipid. The brain lipid that preferentially co-purifies with prions extracted with SMA-MA from prion-infected mice or hamsters is PE, which represents 30.4 % and 33.5 % of the total associated lipid in the resulting nanoparticles, respectively, underscoring its role in mediating accelerated prion propagation (Deleault et al., 2012). This is followed closely by phosphatidylcholine (PC) at 29.9 and 31.3 %, respectively, reflecting its abundance in the outer leaflet of the plasma membrane. The high levels of these lipids are mirrored by those in SMA(2:1)-based prion

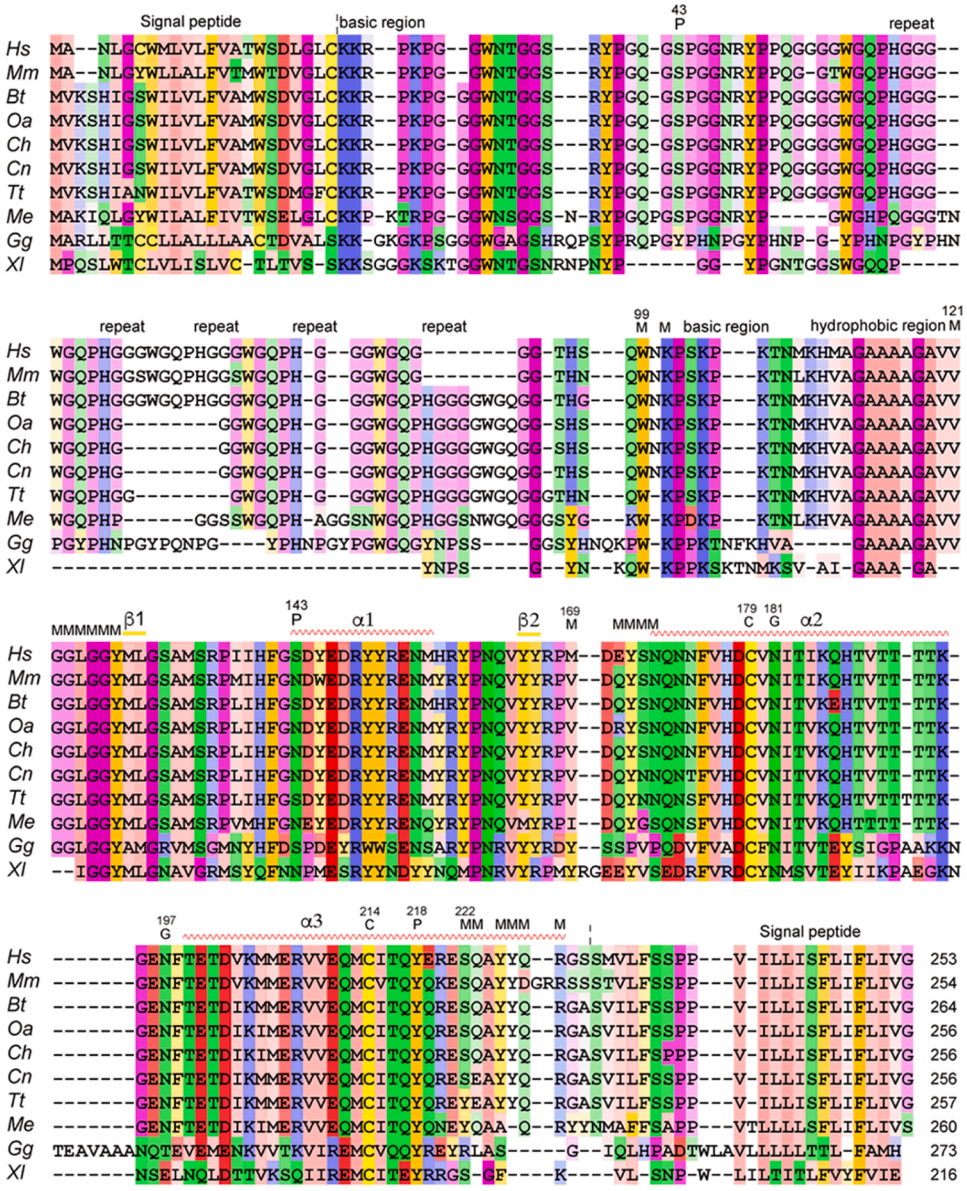

Fig. 3. Alignment of PrP Sequences. Glycosylated (G), phosphorylated (P), cystine (C), membrane interacting (M) residues and secondary structures are indicated above the alignments, along with signal peptide, β strand and α helix numbering. The sequences were aligned with Clustal Omega (Sievers et al., 2011) and coloured with Jalview (Waterhouse et al., 2009). The genus and species are indicated as Hs, *Homo sapiens* (human); Mm, *Mus musculus* (mouse); Bt, *Bos taurus* (bovine); Oa, *Ovis aries* (sheep); Ch, *Capra hircus* (goat); Cn, *Cervus elaphus nelsoni* (elk); Tt, *Tursiops truncatus* (dolphin); Me, *Macropus eugenii* (wallaby); Gg, *Gallus gallus* (chicken); and Xl, *Xenopus laevis* (African clawed frog).

nanoparticles. In contrast SMA(3:1) and sarkosyl remove more PE in particular. The third most abundant prion-associated lipid is cholesterol (20.1 and 13.4 %), followed by PS (11.6 and 10.5 %) and phosphatidylinositol (PI, 4.0 and 5.6 %), which can also stimulate aggregation of recombinant PrP (Tsiroulnikov et al., 2009), and then sphingomyelin at 1.9 % and 1.4 % in mice and hamster-derived prion SMA-MA nanoparticles, respectively. The lipids that are associated with prions extracted from brain reflect their prevalence during the course of disease progression (Guan et al., 1996) as well as their previously documented roles, particularly in the case of PE, in binding to prions in the outer leaflet of the plasmalemma and controlling propagation.

The profile of lipids retained by prions contrasts with those obtained from nanoparticles from other cells. Solubilization of mouse T cells using SMA(3:1) copolymer generates 250 nm membrane fragments enriched in GPI-anchored proteins and Src family kinases as well as smaller nanodiscs (Angelisová et al., 2019). The 13 nm native nanodiscs contain more PC, about 40 %, and about 25 % PE and 10 % PI, and trace amounts of PS, and lower amounts of cholesterol and sphingomyelins than the larger membrane fragments. The extraction of three E. coli proteins, ZipA, FtsA and PdgB, from *E. coli* membranes using SMA(2:1) reveals little or no bias by the copolymer for specific phospholipids based on mass spectrometry analysis (Teo et al., 2019). However the different proteins display distinct preferences for mono-unsaturated phospholipid species in both the PE and PG classes and lipid chain lengths and degrees of unsaturation. Hence lipid composition can be measured quantitatively in nanodiscs and may reflect mechanistic differences of the contained memteins. Such differences in lipid profiles can reflect differences between wild-type and mutant protein activities. This was demonstrated by *in vivo* measurement of lipidomes in *C. elegans* using SMA(3:1) copolymer. In particular the levels of ether-linked lipid levels are dependent on the presence of a functional alkylglycerol monooxygenase enzyme that degrades these lipids (Bada Juarez et al., 2019). Large assemblies of proteins such as those of the metabolon can also be purified together using SMA for identification of the various interacting proteins including peripheral membrane partners, as demonstrated for the machinery responsible for the synthesis of the metabolite dhurrin in sorghum (Laursen et al., 2016). Together these studies demonstrate the general utility of SMALPs for relatively unbiased and accurate identification of co-associated native lipids and proteins as isolated into nanoparticles from endogenous tissues.

Parallels between prion and other neurodegenerative diseases can be drawn, as they have mechanistic relationships including analogous lipid

interactions with acidic phospholipids and gangliosides and can influence each other through cross-seeding (Perissinotto et al., 2019; Ivanova et al., 2020). The α-synuclein protein interacts with membranes in brain where it normally senses physiological changes at nerve terminals. Its formation of cytotoxic prefibrillar oligomers and β-rich amyloid fibrils contributes to the development of Parkinson's disease. The membrane binding mechanism of α-synuclein involves KTKEGV repeats, formation of amphipathic helices and engagement acidic phospholipids and GM1 ganglioside (Perissinotto et al., 2019). The presence of cholesterol in membranes of nanodiscs formed with SMA(2:1) copolymer inhibits binding but promotes fibrillation of α-synuclein, where it may nucleate protein oligomerization (Jakubec et al., 2020). Nanodiscs produced with diisobutylene/maleic acid (DIBMA) copolymer (Fig. 3) are particularly well-suited to resolving its dynamic bilayer binding by circular dichroism (CD) spectroscopy due to the low UV absorbance of this copolymer (Adao et al., 2020). Human, elephant and whale α-synuclein all adopt α-helical structures as they bind PS-enriched bilayers either in the gel and fluid phases of the lipid bilayers. The equilibrium between two populations. *i.e.* the flexible form in solution and helical form on the surface, and can be measured using this approach. The helical structure is temperature dependent, peaking at 35.8 °C, and requires acidic phospholipids, being enhanced by increasing PS levels. The DIBMA copolymer also interacts with α-synuclein and induces helical structure in the absence of lipid. Saturation transfer difference (STD) NMR spectra of nanodisc interactions reveal that α-synuclein binds the polar headgroups of PS and PC lipids as well as the aliphatic group of the polymer. The α-synuclein tetramer is also thought to form a tetramer that acts as a ferrireductase enzyme which maintains Fe^{2+} levels inside cells. However, this activity could not be captured by SMA(3:1) copolymer on PC-containing nanodiscs, despite stabilization of its helical structure (McDowall et al., 2017), potentially due to the acidic copolymer directly binding to the Fe^{2+} or protein or the lack of associated acidic phospholipids. Hence the development of membrane solubilizing polymers that are less "sticky" or charged may be needed to minimize any spurious nonspecific interactions. Nanodiscs formed with MSPs are also useful for detecting acidic phospholipid binding residues and affinities of α-synuclein using NMR and biolayer interferometry methods (Viennet et al., 2018), which in addition to novel SMA derivatives provides further tools to resolve bilayer complexes.

Copolymers developed to broaden the solubility range of nanodiscs include the positively charged SMA-QA, which contains a quaternary ammonium group (Fig. 3). Like negatively charged SMA, it also converts vesicles into nanodiscs with 10–30 nm diameters but is active at pH values from 2 to 10 in the presence of high polyvalent cations concentrations (Ravula et al., 2018). Another basic copolymer, SMI, contains dimethylaminopropyl sidechains on the maleimide group and is soluble below pH 7.8 irrespective of the presence of Mg^{2+} or Ca^{2+} (Hall et al., 2018). In contrast, conventional SMA copolymers are most active at or above pH 7 due to their negative charge and precipitate in millimolar concentrations of divalent cations, which interact with the maleic acid groups. The SMI-based nanodiscs have 6 nm diameters and are stable up to 80 °C and have proven useful for solubilizing and purifying the active human adenosine A_{2A} and V1a vasopressin receptors from human embryonic kidney (HEK) 293 cells and ZipA protein from *E. coli*. A zwitterionic SMA (zSMA) copolymer offers utility under a wide range of buffer, pH and polycation levels, and solubilizes membranes as effectively as conventional SMA copolymers (Fiori et al., 2017). Larger nanodiscs with diameters of up to 50 nm can be made using a short SMA (1.3:1) copolymer containing polar ethanolamine sidechains (Ravula et al., 2017b). The resulting SMA-EA nanodiscs are stable over a broad range of pH and divalent cation levels, and revealed structural features of the cytochrome *b5* protein by NMR. A zwitterionic version of this SMA backbone with ethylenediamine groups called SMA-ED solubilizes vesicles outside the pH range of 5–7 (Ravula et al., 2017a). A dehydration reaction can be used to convert this copolymer to SMAd-A, which solubilizes vesicles below pH 6. This expanding range of copolymers offers the ability to solubilize proteins that bind polyvalent cations or operate at extreme pH values, which may be useful for isolating and characterizing active prions or growing oligomers or fibrils within larger discs.

The universe of amphiphilic copolymers available to form native nanodiscs continues to grow. The high performance of SMA(2:1) polymers inspired testing of a set of methylated stilbene maleic acid (STMA) analogs (Fig. 3). These offer the advantages of strictly alternating subunits on a more rigid backbone, tolerances of Ca^{2+} up to 5−7 mM, and aqueous solubilities between pH 5–10. They also offer higher efficiency solubilization, with only half the concentration of STMA copolymer being needed to gently solubilize both PagP monomers and dimers from *E. coli* outer membranes compared to SMA(2:1) copolymer (Esmaili et al., 2020a). The homogeneous STMA copolymers yield more regular native nanodiscs that are 20 nm in diameter discs and can be used to purify PagP protein by immobilized metal affinity and size exclusion chromatography, suggesting the ability to purify and resolve more memteins at higher resolution once production is scaled.

A set of simpler alternating copolymers composed of acrylic acid and styrene are compatible with up to 7 mM Ca^{2+} and pH > 7. These AASTY copolymers (Fig. 3) solubilize human transient receptor potential melastatin type 4 fused to StrepTagII and green fluorescent protein from mammalian cells. However, these copolymers tend to exclude negatively charge lipid and cholesterol, with a relative subunit ratio of 45:55 for acrylic acid and styrene providing the best performance overall. Protein purification with AASTY benefits from the presence of 250 mM L-arginine to reduce nonspecific ionic interactions but generates lower protein yields and nanoparticle heterogeneity, thus limiting utility for high resolution cEM analysis. Such studies are guiding the development of neutral copolymers to reduce undesirable non-specific interactions and broaden utility to more mammalian targets and labile memteins.

A series of polymethacrylate (PMA) random copolymers spontaneously convert PC-based liposomes and *E. coli* membranes into fragments and nanoparticles (Yasuhara et al., 2017). The cationic PMA copolymer is useful for CD, fluorescence and UV/vis spectroscopy studies, as demonstrated by analysis of the stabilization of a helical intermediate state of the human islet amyloid polypeptide, while suppressing its formation of amyloid fibrils (Sahoo et al., 2019b). A series of inexpensive alkyl polyacrylic acid (APAA) copolymers allow solubilization of dimyristoyl PC (DMPC) vesicles into nanodiscs, and show that those with a *n*-hexyl sidechain are most effective at solubilizing *E. coli* membranes (Hardin et al., 2019). This reveals that longer alkyl sidechains perturb the lipid bilayer more and reduce copolymer solubility in the presence of divalent cations. The development of this array of copolymers is providing structure-activity insights for the design of further improvements to polymer activity, and offers opportunities for solubilizing complex membrane assemblies for determination of improved structures. In the meantime, a variety of membrane binding sites can be predicted computationally from the existing structures and flexible regions, as outlined below.

4. Lipid interaction sites in prion structures

The many structural and functional studies of prion proteins reveal the presence of multiple membrane interaction motifs. At the N-terminus is an unstructured basic-hydrophobic region, which spans the K^{23}RPK motif and contributes to GPCR binding (Kuffer et al., 2016). Here this element is predicted to be membrane interactive (Fig. 1) based on analysis by the BH program (Brzeska et al., 2010). Consistent with this is the apparent insertion of this element into micelles and a posited role in cell penetration (Magzoub et al., 2006) and in prion toxicity of an internally deleted form of PrP (Westergard et al., 2011). Multiple tryptophan residues in the octapeptide repeats between residues 60–91 interact with dodecylphosphocholine (DPC) micelles either in the presence or absence of Cu^{2+} based on NMR analysis of micelle titrations into full length human prion protein and peptides, suggesting that they insert into membranes (Dong et al., 2007). The protonation of the

histidines in these repeats within the low pH environments of endocytic compartments could favor interactions with acidic lipids such as PS (Morillas et al., 1999) while precluding the binding of Cu^{2+} seen at the cell surface. The W^{99}NK motif, which abuts a polybasic motif, is consistently predicted in the results presented here (Figs. 4, 5) to interact with acidic lipid surfaces in PrP solution structures. This is based on analysis by the Membrane Optimal Docking Area (MODA) program (Kufareva et al., 2014), which has been used to identify several novel membrane interaction sites in various proteins (Bissig et al., 2013; Bryant et al., 2020). A hydrophobic region between this element and the structural domain is thought to span intracellular membranes in two orientations and may be critical for conformational regulation (Roseman et al., 2020) as well as the conversion of the helical to the amyloid-forming aggregates (Luhrs et al., 2006). These membrane interacting elements are in regions that lack independently folded structure and could mediate pH-dependent association with acidic phospholipid bilayers *via* relatively non-stereospecific electrostatic and hydrophobic interactions.

The C-terminal half of the prion protein displays an array of structured elements that could mediate more specific lipid interactions. Three proximal membrane interacting motifs are present in the wildtype PrP domain including V^{122}GGL, which precedes the β1 strand, Y^{169}SN between β2 and α2, and Y^{225}YQR in α3. These converge in the 3D structure to form a single continuous surface, which is predicted here to be positioned for membrane binding in most human PrP solution structures (Figs. 4A, 5) based on our MODA analysis. This predicted site is supported by independent studies. The first motif preceding β1 is sensitive to the addition of DPC micelles, as evidenced by chemical shift perturbations, indicating induction of local helical character and membrane insertion; local mutations here enhance the interactions with this membrane mimic (Hornemann et al., 2009), as would biological lipid ligands. The latter two motifs at the α2 and α3 termini are also implicated in ganglioside binding by the hamster prion protein (Sanghera et al., 2011). Together this confirms these three membrane interaction elements, which form a single binding surface. While the proximal C-terminal GPI anchor mediates interactions with lipid rafts, which are enriched in cholesterol, gangliosides and sphingomyelin, and N-terminal sequences can also engage membrane mimics, these do not appear to be essential for formation of infectious isoforms of PrP (Rogers et al., 1993). Instead it is the PrP structural domain that appears to be most critical, and hence the structured membrane binding surface identified here may be particularly crucial for PrP^{Sc} formation in specific membrane environments. The multiplicity of sites that can engage lipids and interface the prion protein with bilayers are likely relevant to the biological function of PrP. These motifs are highly conserved in prion proteins, particularly in the mammals that are prone to prion disease (Fig. 3), suggesting that multivalent membrane binding is an inseparable and longstanding contributor to prion function. There is a divergence of sequences including membrane binding motifs in PrP proteins of species unaffected by prion diseases, suggesting that membrane interactions may play a determining role in propagation.

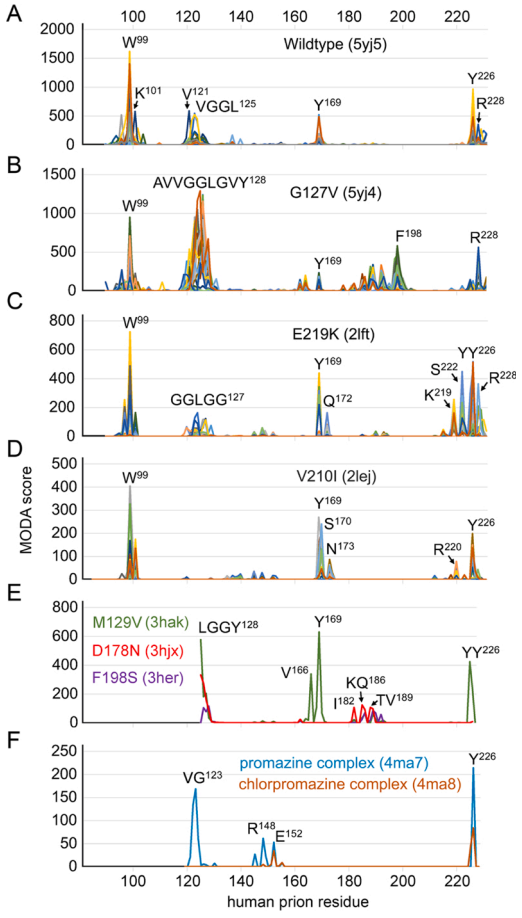

Fig. 4. Membrane binding residues of prions. Human PrP residues consistently having MODA scores of over 30 (Kufareva et al., 2014) in the twenty solution structures of the wildtype protein are labelled (a) as well as some polymorphic and point mutant forms including G127 V (b), E219 K (c) V210I (d), three crystal structures of variant M129 V as well as D178 N and F198 (e) mutants derived from it, and also of two drug molecule complexes (f), as depicted in Fig. 5.

Structures of pathogenic and resistant mutant prion proteins suggest that enhancing the normal membrane binding mode of PrP^{C} is generally protective while promoting dissociation can be deleterious, inducing a variety of prion disease phenotypes. Comparison of structures of the wild-type and G127 V mutant, which confers resistance to several types of prion infections (Asante et al., 2015), shows that a local conformational change of Tyr^{128}, Gly^{131} and Tyr^{163} is induced as well as redistribution of surface electrostatic potentials (Zheng et al., 2018). Analysis of the 20 conformers of the wild-type *vs* mutant proteins indicates that the latter favors membrane interactions particularly *via* the V^{122}GGLGGYM motif, benefiting from the additional exposed hydrophobicity of the Val^{127} sidechain (Figs. 4B, 5). The high frequency M129 V polymorphism modulates timing and neurologic manifestation of human prion diseases (Palmer et al., 1991; Kim et al., 2018), with crystal structures of this form showing the exposed position of V^{129} (Lee et al., 2010) and the three proximal membrane binding elements by the ends of β1, α2 and α3 as seen by NMR (Figs. 4E, 5). Similarly the naturally occurring E219 K prion polymorphism, which confers resistance to sporadic CJD based on *in vitro* and mouse studies, induces alterations in the structure, dynamics and surface charge distribution although downstream effects remain unknown (Biljan et al., 2012a). Here, the membrane interactions of the α3 site are predicted to be enhanced in this mutant based on MODA analysis of the ensemble of 20 NMR structures, with Tyr^{218}, Lys^{219}, Ser^{222} being additionally involved as well as the proximal Gln^{172} and C-terminal YYQRG motif (Figs. 4C, 5). In contrast, the pathological V210I mutation, which is responsible for cases of genetic CJD (gCJD), reduces the likelihood of membrane interactions. The bulkier isoleucine induces conformational changes (Biljan et al., 2012b) and the membrane binding propensity of the site by the β1 site disappears based on MODA analysis (Figs. 4D, 5). The D178 N mutation contributes to the development of fatal familial insomnia or gCJD, depending on whether M129 or V129, respectively, are in *cis* to Asn at codon 178 (Kim et al. reference again). This residue is next to the disulfide bond and its mutation alters the local conformation including of the membrane binding element that precedes the α2 helix (Lee et al., 2010) and dramatically reduces the membrane binding propensity, particularly at the β2 and β3 termini (Figs. 4E, 5). The F198S mutation is associated with GSS disease and leads to exposure of this normally buried sidechain. The crystal structures of this mutant form (Lee et al.,

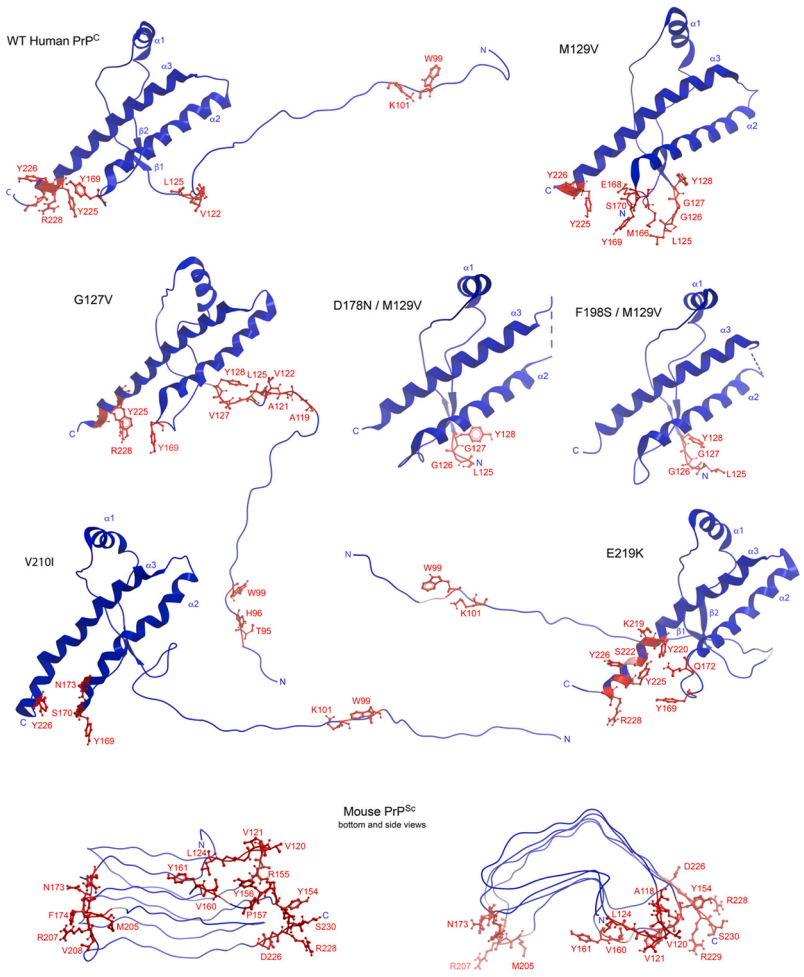

Fig. 5. Membrane interaction sites in prion protein structures. The prion protein residues predicted to be membrane binding in structures based on our MODA analysis are shown. Representatives of ensembles of NMR solution structures of the wildtype human PrP domain (PDB ID: 5yj5) and point mutants including G127 V (5yj4), E219 K (2lft), V210I (2lej) as well as crystal structures of mutants M129 V (3hak), D178 N/M129 V (3hjx), F198S/M129 V (3her) and a model of mouse PrP^{Sc} in two perspectives (Spagnolli et al., 2019) with N and C termini labelled. Membrane interacting residues in consensus sites are shown in red with sidechains and residue labels where MODA scores of at least 30 were calculated (Kufareva et al., 2014). The membrane:PrP complexes would be predicted to involve interaction of the elements shown in red into the lipid bilayer, with their aromatic and hydrophobic groups inserting deeply, and their basic residues engaging acidic lipid headgroups.

2010) reveal altered conformations of the loop and packing between β1, α2 and α3 elements, with even lower membrane binding propensities (Figs. 4E, 5). This suggests that mutations that compromise PrP^{C}:membrane interactions generally predispose to neurodegenerative disease, perhaps by destabilizing the memtein and thus allowing faster conversion, while mutations that support PrP^{C}-membrane binding endow resistance to disease, presumably by stabilizing its functionally intact state. Further analysis of how the various mutations influence the assembly, stability, processing and degradation of PrP-membrane assemblies could shed light on their effects on the predisposition and progression of various prion diseases.

Consistent conformational differences are apparent between the cellular and pathogenic prion forms. When the GPI anchor is cleaved from PrP^{C} by PI-PLC the prion protein becomes particularly prone to conversion into the infectious form based on analysis in cell-free assays (Baron et al., 2002), and the discovery of pathogenic stop codon mutations at Y226X and Q227X (Jansen et al., 2010). This released state simultaneously retains a GPI-independent ability to associate with membranes (Baron and Caughey, 2003), indicating additional sites for membrane binding. The pathogenic form is resistant to release from lipid membranes by PI-PLC as well as partially protected against cleavage by proteases (Borchelt et al., 1990; Stahl et al., 1990; Caughey et al., 1991), suggesting higher avidity interactions between the multimeric state and membrane surfaces. The interaction of recombinant prion protein with PS-containing vesicles orders the octapeptide repeat region that contains membrane-inserting tryptophan residues while destabilizing the C-terminal structured domain, particularly at pH 5 where PS binds best (Morillas et al., 1999). This suggests that both halves of the protein offer somewhat distinct membrane binding surfaces. The entire region between residues ~89 and 227 appears to be structured in the infectious form of the recombinant mouse PrP, while there is less order in the region up to residue ~167 in a noninfectious state based on mass spectrometry analysis of the protein only forms (Li et al., 2018). A cofactor mixture which contains PE lipid and templates rapid propagation protects the membrane-interacting region between residues 91–110 as well as the normally the solvent exposed region encompassing residues 144–163 of the mouse prion (Noble et al., 2015). This suggests a substantial change in conformation during conversion of PrP^{C} into PrP^{Sc} competent forms.

The altered conformations such as β-rich structures formed as prion proteins oligomerize and fibrillize could lead to presentation of a series of different lipid engagements and possible disruption of membranes rather than the dynamic, partial insertion into the bilayer of the cellular form. Indeed, a recent model of the 4-rung β-solenoid of mouse Prp^{Sc} (Spagnolli et al., 2019) displays even more substantial membrane binding propensities of residues in the $AGAVVGGL^{124}$,$YRYP^{157}$, VY^{161}, NF^{174}, $MERV^{208}$ and $DGRRS^{230}$ elements. Only the first and last of these overlap membrane binding elements identified here in PrP^{C} structures, suggesting that they may engage first during the conversion process while the other interactions could follow in a manner that depends on structural rearrangements. All of these PrP^{Sc} membrane binding elements coalesce to form two large, exposed, continuous and proximal ridges along the convex surface of the monomer (Fig. 5), suggesting much stronger bilayer interactions by these subunits than in PrP^{C}. Moreover these ridges are extended by formation of multimers, such that even more substantial interactions with the bilayer would form as

oligomers grow. This model suggests that these membrane docking surfaces may organize the collection and assembly of β-rich subunits, thus accelerating propagation. The lipid bilayer interactions of the β solenoid structure would allow access to known sites for *in vitro* cleavage of PrP^{Sc} preparations (Sevillano et al., 2018). That is, cleaved residues A^{116}, M^{133}/S^{134}, G^{141}, N^{152}/M^{153}, Y^{162} and V^{179} are not predicted to be membrane interactive, and while G^{118} is, it is potentially dynamic and exposed, being on the border of the structured membrane docking site formed by the $VVGGL^{124}$ motif. Hence the membrane-bound orientation of PrP^{Sc}, as proposed here, is consistent with the known proteolytic accessibility of both recombinant and endogenous infectious prions. Moreover, the proposed membrane binding could also explain the inaccessibility of PrP^{Sc} to cleavage by PI-PLC (Stahl et al., 1990).

Strategies for therapeutic intervention can be envisaged including stabilization of PrP^{C}'s membrane bound state, or inhibition of membrane binding by the PrP^{Sc} state. Towards this goal, crystal structures reveal how promazine and chlorpromazine interact with the human PrP^{C} structure *via* similar hydrophobic surface albeit in different poses (Baral et al., 2014). The overall PrP domain structure remains unperturbed, with these compounds docking to and potentially stabilizing the membrane binding elements preceding the β1 strand and in the β2-α2 loop. This reduces the membrane binding propensities here, particularly in the β2-α2 site (Fig. 4F) and could also lead to altered conformations and initiation of fibril formation. Further work is needed as these drug molecules bind weakly to soluble recombinant PrP (Stincardini et al., 2017), they require long, flexible hydrophobic chains to display activity (Korth et al., 2001) and could potentially also engage membranes. Nonetheless, the wealth of structural information and assayable complexes suggests avenues form improving efficacy.

While this study has focused on human PrP, the mechanisms of many other prions could be similarly illuminated. Doppel (Dpl) is a member of the PrP superfamily (Moore et al., 1999) with a generally similar fold for its globular domain, albeit with two disulphide bonds (Mo et al., 2001), and potentially analogous endoproteolytic processing events (Mays et al., 2014). Analysis of Dpl's 3D structures by MODA also reveals a membrane interaction site, albeit distinct from that of PrP (data not shown). Fungal proteins such as the *Saccharomyces cerevisiae* protein Sup35, which is cytosolic and is structurally unrelated to mammalian proteins, also forms self-templating protein aggregates *via* a distinct N-terminal domain. Like mammalian prions, Sup35 also associates with membrane-bound vesicles, suggesting that lipid-dependent dissemination routes of the aggregated species may be shared (Liu et al., 2016). Many other proteins form amyloid assemblies that can favor association with membranes (Cawood et al., 2021), suggesting broader implications. Prominent targets include the islet amyloid polypeptide (IAPP), which is implicated in the progression of type 2 diabetes. When stabilized in nanodiscs IAPP forms non-fibrillar β-sheet conformations that interact with the lipid bilayer (Rodriguez Camargo et al., 2017). Also of major interest is the β-amyloid protein, which is centrally involved in the progression of Alzheimer's disease. This protein binds GM1 ganglioside as a monomer but not as an oligomer based on analysis with MSP nanodiscs (Jakubec et al., 2020) and its intermediate states can be trapped on polymer-based nanodiscs (Sahoo et al., 2018a), suggesting that complexed states leading to neurological disease can increasingly be resolved. Caution needs to be exercised, as the peptides used to form some nanodiscs are also known to engage the β-amyloid protein and inhibit its aggregation and fibrillation (Sahoo et al., 2018b), indicating that choice of the appropriate nanodisc system is key.

The structural insights and nanodisc tools described here may help to enable determination of high resolution structures of diverse infectious proteins bound to lipid bilayers. As these formation of these assemblies involves dynamic termini, exposed loops and flexible sidechains that are vulnerable to detergent association, the presence of detergent-free nanodiscs may be essential for resolving the native complexes. This process can be aided by computational tools such as molecular dynamics (MD) simulations of nanodiscs (Sahoo et al., 2019a) and HADDOCK-based modelling, which requires identification of the membrane interacting residues to model protein:bilayer structures and identify specific lipid contacts (Koppisetti et al., 2014; Lenoir et al., 2015; Bryant et al., 2020). The design of improved lead candidates with efficacy in cellular and animal models will likely depend on further development of such models and assay systems to accurately represent the complex states that drive disease progression.

Acknowledgments

Catharine Trieber and Troy Kervin provided helpful discussions on this work. This project has been supported by the Campus Alberta Innovation Program (RCP-12-002C), NSERC Discovery (RGPIN-2018-04994), TMIC and Alberta Prion Research Institute / Alberta Innovates Bio Solutions (201600018) grants awarded to M.O. We thank the members of the SMALP network and Orbiscope for discussions and for sharing their polymers and methods, and Molsoft LLC for making the ICM program (MODA's engine) and MODA available. We apologize to anyone whose results could not be cited due to space limitations.

References

Acevedo-Morantes, C.Y., Wille, H., 2014. The structure of human prions: from biology to structural models-considerations and pitfalls. Viruses 6, 3875–3892.
Adao, R., Cruz, P.F., Vaz, D.C., Fonseca, F., Pedersen, J.N., Ferreira-da-Silva, F., Brito, R. M.M., Ramos, C.H.I., Otzen, D., Keller, S., Bastos, M., 2020. DIBMA nanodiscs keep alpha-synuclein folded. Biochim. Biophys. Acta Biomembr. 1862, 183314.
Alper, T., 1993. The scrapie enigma: insights from radiation experiments. Radiat. Res. 135, 283–292.
Alper, T., Haig, D.A., Clarke, M.C., 1978. The scrapie agent: evidence against its dependence for replication on intrinsic nucleic acid. J. Gen. Virol. 41, 503–516.
Angelisová, P., Ballek, O., Sýkora, J., Benada, O., Čajka, T., Pokorná, J., Pinkas, D., Hořejší, V., 2019. The use of styrene-maleic acid copolymer (SMA) for studies on T cell membrane rafts. Biochim. Biophys. Acta Biomembr. 1861, 130–141.
Asante, E.A., Smidak, M., Grimshaw, A., Houghton, R., Tomlinson, A., Jeelani, A., Jakubcova, T., Hamdan, S., Richard-Londt, A., Linehan, J.M., Brandner, S., Alpers, M., Whitfield, J., Mead, S., Wadsworth, J.D., Collinge, J., 2015. A naturally occurring variant of the human prion protein completely prevents prion disease. Nature 522, 478–481.
Bada Juarez, J.F., O'Rourke, D., Judge, P.J., Liu, L.C., Hodgkin, J., Watts, A., 2019. Lipodisqs for eukaryote lipidomics with retention of viability: Sensitivity and resistance to Leucobacter infection linked to C. elegans cuticle composition. Chem. Phys. Lipids 222, 51–58.
Baral, P.K., Swayampakula, M., Rout, M.K., Kav, N.N.V., Spyracopoulos, L., Aguzzi, A., James, M.N.G., 2014. Structural basis of prion inhibition by phenothiazine compounds. Structure 22, 291–303.
Baron, G.S., Caughey, B., 2003. Effect of glycosylphosphatidylinositol anchor-dependent and -independent prion protein association with model raft membranes on conversion to the protease-resistant isoform. J. Biol. Chem. 278, 14883–14892.
Baron, G.S., Wehrly, K., Dorward, D.W., Chesebro, B., Caughey, B., 2002. Conversion of raft associated prion protein to the protease-resistant state requires insertion of PrP-res (PrP(Sc)) into contiguous membranes. EMBO J. 21, 1031–1040.
Belichenko, P.V., Brown, D., Jeffrey, M., Fraser, J.R., 2000. Dendritic and synaptic alterations of hippocampal pyramidal neurones in scrapie-infected mice. Neuropathol. Appl. Neurobiol. 26, 143–149.
Beriashvili, D., Spencer, N.R., Dieckmann, T., Overduin, M., Palmer, M., 2020. Characterization of multimeric daptomycin bound to lipid nanodiscs formed by calcium-tolerant styrene-maleic acid co-polymer. BBA Biomembranes 1862, 183234.
Biljan, I., Giachin, G., Ilc, G., Zhukov, I., Plavec, J., Legname, G., 2012a. Structural basis for the protective effect of the human prion protein carrying the dominant-negative E219K polymorphism. Biochem. J. 446, 243–251.
Biljan, I., Ilc, G., Giachin, G., Plavec, J., Legname, G., 2012b. Structural rearrangements at physiological pH: nuclear magnetic resonance insights from the V210I human prion protein mutant. Biochemistry 51, 7465–7474.
Bissig, C., Lenoir, M., Velluz, M.C., Kufareva, I., Abagyan, R., Overduin, M., Gruenberg, J., 2013. Viral infection controlled by a calcium-dependent lipid-binding module in ALIX. Dev. Cell 25, 364–373.
Borchelt, D.R., Scott, M., Taraboulos, A., Stahl, N., Prusiner, S.B., 1990. Scrapie and cellular prion proteins differ in their kinetics of synthesis and topology in cultured cells. J. Cell Biol. 110, 743–752.
Botto, L., Cunati, D., Coco, S., Sesana, S., Bulbarelli, A., Biasini, E., Colombo, L., Negro, A., Chiesa, R., Masserini, M., Palestini, P., 2014. Role of lipid rafts and GM1 in the segregation and processing of prion protein. PLoS One 9, e98344.
Bounhar, Y., Zhang, Y., Goodyer, C.G., LeBlanc, A., 2001. Prion protein protects human neurons against Bax-mediated apoptosis. J. Biol. Chem. 276, 39145–39149.
Bryant, J.A., Morris, F.C., Knowles, T.J., Maderbocus, R., Heinz, E., Boelter, G., Alodaini, D., Colyer, A., Wotherspoon, P.J., Staunton, K.A., Jeeves, M., Browning, D. F., Sevastsyanovich, Y.R., Wells, T.J., Rossiter, A.E., Bavro, V.N., Sridhar, P., Ward, D.G., Chong, Z.S., Goodall, E.C.A., Icke, C., Teo, A., Chng, S.S., Roper, D.I.,

Lithgow, T., Cunningham, A.F., Banzhaf, M., Overduin, M., Henderson, I.R., 2020. Structure of dual-BON domain protein DolP identifies phospholipid binding as a new mechanism for protein localization. Elife 9, e62614.
Brzeska, H., Guag, J., Remmert, K., Chacko, S., Korn, E.D., 2010. An experimentally based computer search identifies unstructured membrane-binding sites in proteins: application to class I myosins, PAKS, and CARMIL. J. Biol. Chem. 285, 5738–5747.
Caughey, B., Raymond, G.J., Ernst, D., Race, R.E., 1991. N-terminal truncation of the scrapie-associated form of PrP by lysosomal protease(s): implications regarding the site of conversion of PrP to the protease-resistant state. J. Virol. 65, 6597–6603.
Cawood, E.E., Karamanos, T.K., Wilson, A.J., Radford, S.E., 2021. Visualizing and trapping transient oligomers in amyloid assembly pathways. Biophys. Chem. 268, 106505.
Deleault, N.R., Piro, J.R., Walsh, D.J., Wang, F., Ma, J., Geoghegan, J.C., Supattapone, S., 2012. Isolation of phosphatidylethanolamine as a solitary cofactor for prion formation in the absence of nucleic acids. Proc. Natl. Acad. Sci. U. S. A. 109, 8546–8551.
Dong, S.L., Cadamuro, S.A., Fiorino, F., Bertsch, U., Moroder, L., Renner, C., 2007. Copper binding and conformation of the N-terminal octarepeats of the prion protein in the presence of DPC micelles as membrane mimetic. Biopolymers 88, 840–847.
Esmaili, M., Brown, C.J., Shaykhutdinov, R., Acevedo-Morantes, C., Wang, Y.L., Wille, H., Gandour, R.D., Turner, S.R., Overduin, M., 2020a. Homogeneous nanodiscs of native membranes formed by stilbene-maleic-acid copolymers. Nanoscale 12, 16705–16709.
Esmaili, M., Tancowny, B.P., Wang, X., Wille, H., Overduin, M., 2020b. Infectious lipid-bound prion multimers in custom native nanodiscs. J. Biol. Chem. 295, 8460–8469.
Fiori, M.C., Jiang, Y., Altenberg, G.A., Liang, H., 2017. Polymer-encased nanodiscs with improved buffer compatibility. Sci. Rep. 7, 7432.
Gibbons, R.A., Hunter, G.D., 1967. Nature of the scrapie agent. Nature 215, 1041–1043.
Glatzel, M., Linsenmeier, L., Dohler, F., Krasemann, S., Puig, B., Altmeppen, H.C., 2015. Shedding light on prion disease. Prion 9, 244–256.
Godsave, S.F., Wille, H., Kujala, P., Latawiec, D., DeArmond, S.J., Serban, A., Prusiner, S. B., Peters, P.J., 2008. Cryo-immunogold electron microscopy for prions: toward identification of a conversion site. J. Neurosci. 28, 12489–12499.
Guan, Z., Soderberg, M., Sindelar, P., Prusiner, S.B., Kristensson, K., Dallner, G., 1996. Lipid composition in scrapie-infected mouse brain: prion infection increases the levels of dolichyl phosphate and ubiquinone. J. Neurochem. 66, 277–285.
Haigh, C.L., Tumpach, C., Drew, S.C., Collins, S.J., 2015. The prion protein N1 and N2 cleavage fragments bind to phosphatidylserine and phosphatidic acid; Relevance to stress-protection responses. PLoS One 10, e0134680.
Hall, S., Tognoloni, C., Charlton, J., Bragginton, É., Rothnie, A., Sridhar, P., Wheatley, M., Knowles, T., Arnold, T., Edler, K., TR. D, 2018. An acid-compatible co-polymer for the solubilization of membranes and proteins into lipid bilayer-containing nanoparticles. Nanoscale 10, 10609–10619.
Haraguchi, T., Fisher, S., Olofsson, S., Endo, T., Groth, D., Tarentino, A., Borchelt, D.R., Teplow, D., Hood, L., Burlingame, A., et al., 1989. Asparagine-linked glycosylation of the scrapie and cellular prion proteins. Arch. Biochem. Biophys. 274, 1–13.
Hardin, N.Z., Ravula, T., Mauro, G.D., Ramamoorthy, A., 2019. Hydrophobic functionalization of polyacrylic acid as a versatile platform for the development of polymer lipid nanodisks. Small 15, e1804813.
Hornemann, S., von Schroetter, C., Damberger, F.F., Wuthrich, K., 2009. Prion protein-detergent micelle interactions studied by NMR in solution. J. Biol. Chem. 284, 22713–22721.
Ivanova, M.I., Lin, Y., Lee, Y.H., Zheng, J., Ramamoorthy, A., 2020. Biophysical processes underlying cross-seeding in amyloid aggregation and implications in amyloid pathology. Biophys. Chem. 269, 106507.
Jakubec, M., Barias, E., Furse, S., Govasli, M.L., George, V., Turcu, D., Iashchishyn, I.A., Morozova-Roche, L.A., Halskau, O., 2020. Cholesterol-containing lipid nanodiscs promote an alpha-synuclein binding mode that accelerates oligomerization. FEBS J.
Jansen, C., Parchi, P., Capellari, S., Vermeij, A.J., Corrado, P., Baas, F., Strammiello, R., van Gool, W.A., van Swieten, J.C., Rozemuller, A.J., 2010. Prion protein amyloidosis with divergent phenotype associated with two novel nonsense mutations in PRNP. Acta Neuropathol. 119, 189–197.
Kanaani, J., Prusiner, S.B., Diacovo, J., Baekkeskov, S., Legname, G., 2005. Recombinant prion protein induces rapid polarization and development of synapses in embryonic rat hippocampal neurons in vitro. J. Neurochem. 95, 1373–1386.
Kim, M.O., Takada, L.T., Wong, K., Forner, S.A., Geschwind, M.D., 2018. Genetic PrP prion diseases. Cold Spring Harb. Perspect. Biol. 10, a033134.
Klein, T.R., Kirsch, D., Kaufmann, R., Riesner, D., 1998. Prion rods contain small amounts of two host sphingolipids as revealed by thin-layer chromatography and mass spectrometry. Biol. Chem. 379, 655–666.
Knowles, T.J., Finka, R., Smith, C., Lin, Y.P., Dafforn, T., Overduin, M., 2009. Membrane proteins solubilized intact in lipid containing nanoparticles bounded by styrene maleic acid copolymer. J. Am. Chem. Soc. 131, 7484–7485.
Koppisetti, R.K., Fulcher, Y.G., Jurkevich, A., Prior, S.H., Xu, J., Lenoir, M., Overduin, M., Van Doren, S.R., 2014. Ambidextrous binding of cell and membrane bilayers by soluble matrix metalloproteinase-12. Nat. Commun. 5, 5552.
Korth, C., May, B.C., Cohen, F.E., Prusiner, S.B., 2001. Acridine and phenothiazine derivatives as pharmacotherapeutics for prion disease. Proc. Natl. Acad. Sci. U. S. A. 98, 9836–9841.
Kufareva, I., Lenoir, M., Dancea, F., Sridhar, P., Raush, E., Bissig, C., Gruenberg, J., Abagyan, R., Overduin, M., 2014. Discovery of novel membrane binding structures and functions. Biochem. Cell Biol. 92, 555–563.
Kuffer, A., Lakkaraju, A.K., Mogha, A., Petersen, S.C., Airich, K., Doucerain, C., Marpakwar, R., Bakirci, P., Senatore, A., Monnard, A., Schiavi, C., Nuvolone, M., Grosshans, B., Hornemann, S., Bassilana, F., Monk, K.R., Aguzzi, A., 2016. The prion protein is an agonistic ligand of the G protein-coupled receptor Adgrg6. Nature 536, 464–468.
Latarjet, R., Muel, B., Haig, D.A., Clarke, M.C., Alper, T., 1970. Inactivation of the scrapie agent by near monochromatic ultraviolet light. Nature 227, 1341–1343.
Lauren, J., Gimbel, D.A., Nygaard, H.B., Gilbert, J.W., Strittmatter, S.M., 2009. Cellular prion protein mediates impairment of synaptic plasticity by amyloid-beta oligomers. Nature 457, 1128–1132.
Laursen, T., Borch, J., Knudsen, C., Bavishi, K., Torta, F., Martens, H.J., Silvestro, D., Hatzakis, N.S., Wenk, M.R., Dafforn, T.R., Olsen, C.E., Motawia, M.S., Hamberger, B., Møller, B.L., Bassard, J.-E., 2016. Characterization of a dynamic metabolon producing the defense compound dhurrin in sorghum. Science 354, 890–893.
Lee, S., Antony, L., Hartmann, R., Knaus, K.J., Surewicz, K., Surewicz, W.K., Yee, V.C., 2010. Conformational diversity in prion protein variants influences intermolecular beta-sheet formation. EMBO J. 29, 251–262.
Lee, S.C., Knowles, T.J., Postis, V.L., Jamshad, M., Parslow, R.A., Lin, Y.P., Goldman, A., Sridhar, P., Overduin, M., Muench, S.P., Dafforn, T.R., 2016. A method for detergent-free isolation of membrane proteins in their local lipid environment. Nat. Protoc. 11, 1149–1162.
Leighton, P.L.A., Nadolski, N.J., Morrill, A., Hamilton, T.J., Allison, W.T., 2018. An ancient conserved role for prion protein in learning and memory. Biol. Open 7 bio025734.
Lenoir, M., Grzybek, M., Majkowski, M., Rajesh, S., Kaur, J., Whittaker, S.B., Coskun, U., Overduin, M., 2015. Structural basis of dynamic membrane recognition by trans-Golgi network specific FAPP proteins. J. Mol. Biol. 427, 966–981.
Levine, D.J., Stohr, J., Falese, L.E., Ollesch, J., Wille, H., Prusiner, S.B., Long, J.R., 2015. Mechanism of scrapie prion precipitation with phosphotungstate anions. ACS Chem. Biol. 10, 1269–1277.
Li, Q., Wang, F., Xiao, X., Kim, C., Bohon, J., Kiselar, J., Safar, J.G., Ma, J., Surewicz, W. K., 2018. Structural attributes of mammalian prion infectivity: insights from studies with synthetic prions. J. Biol. Chem. 293, 18494–18503.
Lindhoud, S., Carvalho, V., Pronk, J.W., Aubin-Tam, M.E., 2016. SMA-SH: modified styrene-maleic acid copolymer for functionalization of lipid nanodiscs. Biomacromolecules 17, 1516–1522.
Liu, S., Hossinger, A., Hofmann, J.P., Denner, P., Vorberg, I.M., 2016. Horizontal transmission of cytosolic Sup35 prions by extracellular vesicles. mBio 7.
Luhrs, T., Zahn, R., Wuthrich, K., 2006. Amyloid formation by recombinant full-length prion proteins in phospholipid bicelle solutions. J. Mol. Biol. 357, 833–841.
Magzoub, M., Sandgren, S., Lundberg, P., Oglecka, K., Lilja, J., Wittrup, A., Goran Eriksson, L.E., Langel, U., Belting, M., Graslund, A., 2006. N-terminal peptides from unprocessed prion proteins enter cells by macropinocytosis. Biochem. Biophys. Res. Commun. 348, 379–385.
Mays, C.E., Coomaraswamy, J., Watts, J.C., Yang, J., Ko, K.W., Strome, B., Mercer, R.C., Wohlgemuth, S.L., Schmitt-Ulms, G., Westaway, D., 2014. Endoproteolytic processing of the mammalian prion glycoprotein family. FEBS J. 281, 862–876.
McDowall, J.S., Ntai, I., Hake, J., Whitley, P.R., Mason, J.M., Pudney, C.R., Brown, D.R., 2017. Steady-state kinetics of α-Synuclein ferrireductase activity identifies the catalytically competent species. Biochemistry 56, 2497–2505.
Miller, M.B., Wang, D.W., Wang, F., Noble, G.P., Ma, J., Woods Jr, V.L., Li, S., Supattapone, S., 2013. Cofactor molecules induce structural transformation during infectious prion formation. Structure 21, 2061–2068.
Mo, H., Moore, R.C., Cohen, F.E., Westaway, D., Prusiner, S.B., Wright, P.E., Dyson, H.J., 2001. Two different neurodegenerative diseases caused by proteins with similar structures. Proc. Natl. Acad. Sci. U. S. A. 98, 2352–2357.
Moore, R.C., Lee, I.Y., Silverman, G.L., Harrison, P.M., Strome, R., Heinrich, C., Karunaratne, A., Pasternak, S.H., Chishti, M.A., Liang, Y., Mastrangelo, P., Wang, K., Smit, A.F., Katamine, S., Carlson, G.A., Cohen, F.E., Prusiner, S.B., Melton, D.W., Tremblay, P., Hood, L.E., Westaway, D., 1999. Ataxia in prion protein (PrP)-deficient mice is associated with upregulation of the novel PrP-like protein doppel. J. Mol. Biol. 292, 797–817.
Morillas, M., Swietnicki, W., Gambetti, P., Surewicz, W.K., 1999. Membrane environment alters the conformational structure of the recombinant human prion protein. J. Biol. Chem. 274, 36859–36865.
Naslavsky, N., Shmeeda, H., Friedlander, G., Yanai, A., Futerman, A.H., Barenholz, Y., Taraboulos, A., 1999. Sphingolipid depletion increases formation of the scrapie prion protein in neuroblastoma cells infected with prions. J. Biol. Chem. 274, 20763–20771.
Noble, G.P., Wang, D.W., Walsh, D.J., Barone, J.R., Miller, M.B., Nishina, K.A., Li, S., Supattapone, S., 2015. A structural and functional comparison between infectious and non-infectious autocatalytic recombinant PrP conformers. PLoS Pathog. 11, e1005017.
Oluwole, A.O., Danielczak, B., Meister, A., Babalola, J.O., Vargas, C., Keller, S., 2017. Solubilization of membrane proteins into functional lipid-bilayer nanodiscs using a diisobutylene/maleic acid copolymer. Angew. Chem. Int. Ed. Engl. 56, 1919–1924.
Overduin, M., Esmaili, M., 2019a. Memtein: the fundamental unit of membrane-protein structure and function. Chem. Phys. Lipids 218, 73–84.
Overduin, M., Esmaili, M., 2019b. Structures and interactions of transmembrane targets in native nanodiscs. SLAS Discov. 24, 943–952.
Palmer, M.S., Dryden, A.J., Hughes, J.T., Collinge, J., 1991. Homozygous prion protein genotype predisposes to sporadic Creutzfeldt-Jakob disease. Nature 352, 340–342.
Pan, K.M., Baldwin, M., Nguyen, J., Gasset, M., Serban, A., Groth, D., Mehlhorn, I., Huang, Z., Fletterick, R.J., Cohen, F.E., et al., 1993. Conversion of alpha-helices into beta-sheets features in the formation of the scrapie prion proteins. Proc. Natl. Acad. Sci. U. S. A. 90, 10962–10966.
Perissinotto, F., Rondelli, V., Parisse, P., Tormena, N., Zunino, A., Almasy, L., Merkel, D. G., Bottyan, L., Sajti, S., Casalis, L., 2019. GM1 Ganglioside role in the interaction of

Alpha-synuclein with lipid membranes: Morphology and structure. Biophys. Chem. 255, 106272.
Ravula, T., Hardin, N.Z., Ramadugu, S.K., Ramamoorthy, A., 2017a. PH tunable and divalent metal ion tolerant polymer lipid nanodiscs. Langmuir 33, 10655–10662.
Ravula, T., Ramadugu, S.K., Di Mauro, G., Ramamoorthy, A., 2017b. Bioinspired, size-tunable self-assembly of polymer–Lipid bilayer nanodiscs. Angew. Chem. Int. Ed. Engl. 56, 11466–11470.
Ravula, T., Hardin, N.Z., Ramadugu, S.K., Cox, S.J., Ramamoorthy, A., 2018. Formation of pH-Resistant monodispersed polymer-lipid nanodiscs. Angew. Chem. Int. Ed. Engl. 57, 1342–1345.
Re, F., Sesana, S., Barbiroli, A., Bonomi, F., Cazzaniga, E., Lonati, E., Bulbarelli, A., Masserini, M., 2008. Prion protein structure is affected by pH-dependent interaction with membranes: a study in a model system. FEBS Lett. 582, 215–220.
Riek, R., Hornemann, S., Wider, G., Billeter, M., Glockshuber, R., Wuthrich, K., 1996. NMR structure of the mouse prion protein domain PrP(121-231). Nature 382, 180–182.
Rodriguez Camargo, D.C., Korshavn, K.J., Jussupow, A., Raltchev, K., Goricanec, D., Fleisch, M., Sarkar, R., Xue, K., Aichler, M., Mettenleiter, G., Walch, A.K., Camilloni, C., Hagn, F., Reif, B., Ramamoorthy, A., 2017. Stabilization and structural analysis of a membrane-associated hIAPP aggregation intermediate. Elife 6, e31226.
Rogers, M., Yehiely, F., Scott, M., Prusiner, S.B., 1993. Conversion of truncated and elongated prion proteins into the scrapie isoform in cultured cells. Proc. Natl. Acad. Sci. U. S. A. 90, 3182–3186.
Roseman, G.P., Wu, B., Wadolkowski, M.A., Harris, D.A., Millhauser, G.L., 2020. Intrinsic toxicity of the cellular prion protein is regulated by its conserved central region. FASEB J. 34, 8734–8748.
Sahoo, B.R., Genjo, T., Bekier, M., Cox, S.J., Stoddard, A.K., Ivanova, M., Yasuhara, K., Fierke, C.A., Wang, Y., Ramamoorthy, A., 2018a. Alzheimer's amyloid-beta intermediates generated using polymer-nanodiscs. Chem. Commun. (Camb.) 54, 12883–12886.
Sahoo, B.R., Genjo, T., Cox, S.J., Stoddard, A.K., Anantharamaiah, G.M., Fierke, C., Ramamoorthy, A., 2018b. Nanodisc-forming scaffold protein promoted retardation of amyloid-beta aggregation. J. Mol. Biol. 430, 4230–4244.
Sahoo, B.R., Genjo, T., Moharana, K.C., Ramamoorthy, A., 2019a. Self-assembly of polymer-encased lipid nanodiscs and membrane protein reconstitution. J. Phys. Chem. B 123, 4562–4570.
Sahoo, B.R., Genjo, T., Nakayama, T.W., Stoddard, A.K., Ando, T., Yasuhara, K., Fierke, C.A., Ramamoorthy, A., 2019b. A cationic polymethacrylate-copolymer acts as an agonist for β-amyloid and an antagonist for amylin fibrillation. Chem. Sci. 10, 3976–3986.
Saleem, F., Bjorndahl, T.C., Ladner, C.L., Perez-Pineiro, R., Ametaj, B.N., Wishart, D.S., 2014. Lipopolysaccharide induced conversion of recombinant prion protein. Prion 8, 28939.
Sanghera, N., Correia, B.E., Correia, J.R., Ludwig, C., Agarwal, S., Nakamura, H.K., Kuwata, K., Samain, E., Gill, A.C., Bonev, B.B., Pinheiro, T.J., 2011. Deciphering the molecular details for the binding of the prion protein to main ganglioside GM1 of neuronal membranes. Chem. Biol. 18, 1422–1431.
Schilling, K.M., Tao, L., Wu, B., Kiblen, J.T.M., Ubilla-Rodriguez, N.C., Pushie, M.J., Britt, R.D., Roseman, G.P., Harris, D.A., Millhauser, G.L., 2020. Both N-terminal and C-terminal histidine residues of the prion protein are essential for copper coordination and neuroprotective self-regulation. J. Mol. Biol. 432, 4408–4425.
Sevillano, A.M., Fernandez-Borges, N., Younas, N., Wang, F., S R.E, Bravo, S., Vazquez-Fernandez, E., Rosa, I., Erana, H., Gil, D., Veiga, S., Vidal, E., Erickson-Beltran, M.L., Guitian, E., Silva, C.J., Nonno, R., Ma, J., Castilla, J., J R.R, 2018. Recombinant PrPSc shares structural features with brain-derived PrPSc: insights from limited proteolysis. PLoS Pathog. 14, e1006797.
Simoneau, S., Rezaei, H., Sales, N., Kaiser-Schulz, G., Lefebvre-Roque, M., Vidal, C., Fournier, J.G., Comte, J., Wopfner, F., Grosclaude, J., Schatzl, H., Lasmezas, C.I., 2007. In vitro and in vivo neurotoxicity of prion protein oligomers. PLoS Pathog. 3, e125.
Smith, A.A.A., Autzen, H.E., Faust, B., Mann, J.L., Muir, B.W., Howard, S., Postma, A., Spakowitz, A.J., Cheng, Y., Appel, E.A., 2020. Lipid nanodiscs via ordered copolymers. Chem 6, 2782–2795.
Spagnolli, G., Rigoli, M., Orioli, S., Sevillano, A.M., Faccioli, P., Wille, H., Biasini, E., Requena, J.R., 2019. Full atomistic model of prion structure and conversion. PLoS Pathog. 15, e1007864.
Stahl, N., Borchelt, D.R., Hsiao, K., Prusiner, S.B., 1987. Scrapie prion protein contains a phosphatidylinositol glycolipid. Cell 51, 229–240.
Stahl, N., Borchelt, D.R., Prusiner, S.B., 1990. Differential release of cellular and scrapie prion proteins from cellular membranes by phosphatidylinositol-specific phospholipase C. Biochemistry 29, 5405–5412.
Stahl, N., Baldwin, M.A., Hecker, R., Pan, K.M., Burlingame, A.L., Prusiner, S.B., 1992. Glycosylinositol phospholipid anchors of the scrapie and cellular prion proteins contain sialic acid. Biochemistry 31, 5043–5053.
Stincardini, C., Massignan, T., Biggi, S., Elezgarai, S.R., Sangiovanni, V., Vanni, I., Pancher, M., Adami, V., Moreno, J., Stravalaci, M., Maietta, G., Gobbi, M., Negro, A., Requena, J.R., Castilla, J., Nonno, R., Biasini, E., 2017. An antipsychotic drug exerts anti-prion effects by altering the localization of the cellular prion protein. PLoS One 12, e0182589.
Taraboulos, A., Scott, M., Semenov, A., Avrahami, D., Laszlo, L., Prusiner, S.B., 1995. Cholesterol depletion and modification of COOH-terminal targeting sequence of the prion protein inhibit formation of the scrapie isoform. J. Cell Biol. 129, 121–132.
Teo, A.C.K., Lee, S.C., Pollock, N.L., Stroud, Z., Hall, S., Thakker, A., Pitt, A.R., Dafforn, T.R., Spickett, C.M., Roper, D.I., 2019. Analysis of SMALP co-extracted phospholipids shows distinct membrane environments for three classes of bacterial membrane protein. Sci. Rep. 9, 1813.
Tsiroulnikov, K., Shchutskaya, Y., Muronetz, V., Chobert, J.M., Haertle, T., 2009. Phospholipids influence the aggregation of recombinant ovine prions. From rapid extensive aggregation to amyloidogenic conversion. Biochim. Biophys. Acta 1794, 506–511.
Viennet, T., Wordehoff, M.M., Uluca, B., Poojari, C., Shaykhalishahi, H., Willbold, D., Strodel, B., Heise, H., Buell, A.K., Hoyer, W., Etzkorn, M., 2018. Structural insights from lipid-bilayer nanodiscs link alpha-Synuclein membrane-binding modes to amyloid fibril formation. Commun. Biol. 1, 44.
Watts, J.C., Prusiner, S.B., 2017. Experimental models of inherited PrP prion diseases. Cold Spring Harb. Perspect. Med. 7, a027151.
Westergard, L., Turnbaugh, J.A., Harris, D.A., 2011. A nine amino acid domain is essential for mutant prion protein toxicity. J. Neurosci. 31, 14005–14017.
Yasuhara, K., Arakida, J., Ravula, T., Ramadugu, S.K., Sahoo, B., Kikuchi, J.I., Ramamoorthy, A., 2017. Spontaneous lipid nanodisc fomation by amphiphilic polymethacrylate copolymers. J. Am. Chem. Soc. 139, 18657–18663.
Yost, C.S., Lopez, C.D., Prusiner, S.B., Myers, R.M., Lingappa, V.R., 1990. Non-hydrophobic extracytoplasmic determinant of stop transfer in the prion protein. Nature 343, 669–672.
Zheng, Z., Zhang, M., Wang, Y., Ma, R., Guo, C., Feng, L., Wu, J., Yao, H., Lin, D., 2018. Structural basis for the complete resistance of the human prion protein mutant G127V to prion disease. Sci. Rep. 8, 13211.